The Role of Nde1 Phosphorylation in Interkinetic Nuclear Migration and Neural Migration During Cortical Development

David J Doobin, Paige Helmer, Aurelie Carabalona, Chiara Bertipaglia, Richard B Vallee

The Role of Nde1 Phosphorylation in Interkinetic Nuclear Migration and Neural Migration During Cortical Development

David J Doobin,[1,*] Paige Helmer,[2,*] Aurelie Carabalona,[3] Chiara Bertipaglia,[4] Richard B Vallee[5]

*These authors contributed equally

[1]Massachusetts Eye and Ear, Boston, MA, USA

[2]Zuckerman Mind Brain Behavior Institute, Columbia University, New York, NY, USA

[3]Institute of Mediterranean Neurobiology, Aix-Marseille University, Marseille, France

[4]Wu Tsai Neurosciences Institute, Stanford University, Stanford, CA, USA

[5]Department of Pathology and Cell Biology, College of Physicians and Surgeons, Columbia University, New York, NY, USA

The Role of Nde1 Phosphorylation in Interkinetic Nuclear Migration and Neural Migration During Cortical Development

Abstract

Nde1 is a cytoplasmic dynein regulatory protein with important roles in vertebrate brain development. One noteworthy function is in the nuclear oscillatory behavior in neural progenitor cells, the control and mechanism of which remain poorly understood**.** Nde1 contains multiple phosphorylation sites for the cell cycle-dependent protein kinase CDK1, though the function of these sites is not well understood. To test their role in brain development we expressed phosphorylation-state mutant forms of Nde1 in embryonic rat brains using *in utero* electroporation. We find that Nde1 T215 and T243 phosphomutants block apical interkinetic nuclear migration (INM) and, consequently, mitosis in radial glial progenitor cells. Another Nde1 phosphomutant at T246 also interfered with mitotic entry without affecting INM, suggesting a more direct role for Nde1 T246 in mitotic regulation. We also found that the Nde1 S214F mutation, which is associated with schizophrenia, inhibits Cdk5 phosphorylation at an adjacent residue which causes alterations in neuronal lamination. These results together identify important new roles for Nde1 phosphorylation in neocortical development and disease, and represent the first evidence for Nde1 phosphorylation roles in INM and neuronal lamination.

Significance Statement

Nde1 dysregulation has been reported to play a role in human schizophrenia and possibly other diseases. However, the specific consequences of Nde1 mutations in regulating radial glial progenitor cell behavior during interkinetic nuclear migration and other aspects of brain development remain poorly understood.

This study shows the importance of Nde1 phospho-regulation in rat neocortical development, reporting clear and potent effects of specific Nde1 phospho-mutations in brain development.

The results provide insight into little-understood mechanisms controlling radial glial progenitor cell mitotic entry and reveal a novel post-mitotic role for Nde1 phosphorylation in schizophrenia.

Introduction

Neocortical development is a complex process involving multiple steps in neurogenesis and subsequent post-mitotic neuronal migration. In earlier work, we found that the minus end-directed microtubule motor protein cytoplasmic dynein, and a number of its regulatory proteins, play prominent roles in these behaviors.(Tsai et al. 2010; Baffet, Hu, and Vallee 2015; Doobin et al. 2016) The dynein regulators include LIS1, its interactors Nde1 and Ndel1, and the nuclear pore-binding proteins BicD2 and CENP-F, which are known to be involved in dynein recruitment to the nuclear envelope (NE) (Figure 1). Interference with dynein expression or function, or that of its regulatory proteins, causes a number of brain developmental defects. LIS1 haploinsufficiency causes type I lissencephaly,(Doobin et al. 2016; Reiner et al. 1993; Hirotsune et al. 1998)mutations in Nde1 cause severe forms of microcephaly or microlissencephaly, and mutations in Ndel1 are embryonic lethal.(Doobin et al. 2016; Feng et al. 2000; Pawlisz et al. 2008; Alkuraya et al. 2011; Bakircioglu et al. 2011)

Previous work in our lab revealed that reduced Nde1 expression causes a marked decrease in mitotic index in the radial glial progenitor cells (RGPs),(Doobin et al. 2016) which give rise to most of the neurons in the developing neocortex.(Kriegstein and Alvarez-Buylla 2009) The RGP somata are located within the ventricular zone (VZ) of the developing brain, but also extend highly elongated basal processes spanning the distance from the ventricular to the pial surfaces of the brain and providing scaffolding for neuronal migration and cortical assembly.(Kriegstein and Alvarez-Buylla 2009) RGP nuclei undergo a remarkable form of cell cycle-dependent oscillatory behavior known as interkinetic nuclear migration (INM). During G1, the nucleus travels basally, away from the ventricle, and then, during G2, apically back to the ventricle (Figure 1). We found these behaviors to be driven, respectively, by the kinesin Kif1A, and cytoplasmic dynein.[1] We also found that, for mitosis to proceed, the RGP nucleus must reach the apical terminus of the RGP cell, where the centrosome resides.(Hu et al. 2013) Whether the juxtaposition of centrosome and nucleus is sufficient for mitotic entry or if other conditions must be fulfilled remains uncertain.

Apical INM in RGPs is activated by the G2-specific protein kinase CDK1, which controls dynein recruitment to the RGP nuclear envelope.(Baffet, Hu, and Vallee 2015; Strzyz et al. 2015) One role for CDK1 is to phosphorylate the nucleoporin RanBP2 during early G2,(Splinter et al. 2010) which activates its recruitment of the dynein adaptor BicD2, and, in turn, dynein itself, to the NE.(Hu et al. 2013; Splinter et al. 2012; 2010) As G2 progresses, Cdk1 also phosphorylates Nde1 to activate its recruitment of cytoplasmic dynein to the large NE- and kinetochore-binding scaffold protein CENP-F (Figure 1).(Hu et al. 2013; Wynne and Vallee 2018) This behavior occurs when CENP-F emerges from inside the nucleus and binds to the NE via the nucleoporin Nup133.(Bolhy et al. 2011)

These observations and studies in non-neuronal cells(Splinter et al. 2010; 2012; Wynne and Vallee 2018) have suggested that BicD2-mediated dynein recruitment temporally precedes CENP-F-mediated dynein recruitment, presumably resulting in a gradual increase in apically directed dynein-generated force at at the RGP NE as G2 progresses.(Hu et al. 2013) Consistent with this hypothesis, BicD2 expression can rescue INM in both BicD2- or CENP-F knockdown conditions.(Hu et al. 2013) Curiously, however, BidD2 could not rescue a defect in RGP mitotic

entry caused by Nde1 knockdown.(Doobin et al. 2016) This result suggested that Nde1 might play a unique additional role *directly* in RGP mitotic entry.

In contrast to the clear effects of Nde1 RNAi we have observed on RGP behavior,(Doobin et al. 2016) we found little effect in these cells of RNAi for the Nde1 paralogue Ndel1, but instead a clear inhibitory effect on post-mitotic neuronal migration.(Doobin et al. 2016) The differences in cellular behavior associated with the two orthologues presumably account for observed phenotypic differences *in vivo*. Human NDE1 mutations cause decreased neurogenesis,(Doobin et al. 2016; Feng et al. 2000; Alkuraya et al. 2011) manifesting in a hereditary form of microcephaly, with little reported effect on post-mitotic neuronal behavior. In contrast, a mouse model with a Ndel1 deletion exhibited microlissencephaly,(Wynshaw-Boris et al. 2010) consistent with a more substantial defect in post-mitotic neuronal migration.

Nde1 and Ndel1 each contain multiple sites for CDK1 and CDK5 phosphorylation, though the relative contributions of these sites in controlling cellular and subcellular behavior are incompletely known in general, and in the developing brain in particular. Mutations in Ndel1 at its Cdk1 and Cdk5 phosphorylation sites have been reported to reduce Ndel binding to the G2 NE.(Hebbar et al. 2008) Effects of Ndel1 phosphorylation on lysosome transport have also been reported.(Klinman, Tokito, and Holzbaur 2017; Pandey and Smith 2011) We more recently found pronounced effects of Cdk1 phosphorylation of Nde1 on nucleus and kinetochore recruitment in dividing Hela cells.(Wynne and Vallee 2018) Cdk1 phosphorylation enhanced Nde1 recruitment to the prophase NE and markedly prolonged Nde1 localization at kinetochores, surprisingly into late anaphase. This pattern was strikingly similar to that of the Nde1 interactor CENP-F. Overexpression of wild type (WT) NDE1 or of a triple CDK1 phosphomimetic mutant also resulted in clear decoration of the G2 NE in HeLa cells, while triple phosphomutant NDE1 failed to localize to the NE.(Wynne and Vallee 2018)

Previous studies focused on three residues as phosphorylation sites within the disordered region of Nde1: T215, T243, and T246, all predicted CDK1 phosphorylation sites.(Alkuraya et al. 2011; Wynne and Vallee 2018) Given the previous work implicating these three sites in the recruitment of NDE1 to the NE and the poor conservation of other CDK1 sites, this study focuses on T215, T243, and T246 as potential regulators of NDE1 function in RGPs.(Alkuraya et al. 2011; Hirohashi et al. 2006)

In addition to a role in microcephaly, mutations in NDE1 have been associated with a spectrum of neuropsychiatric diseases, including schizophrenia.(Blackwood et al. 2001; Kimura et al. 2015; Johnstone et al. 2015) Several families with severe microcephaly or microlissencephaly have been found to have homozygous recessive NDE1 deletions which result in either premature truncation of the protein, or no detectable expression.(Alkuraya et al. 2011; Bakircioglu et al. 2011) Copy number variants of NDE1 have also been linked to schizophrenia.(Johnstone et al. 2015) Nde1 is also a known binding partner of DISC1, mutations in which were found to be responsible for the first known heritable form of schizophrenia.(Blackwood et al. 2001; St Clair et al. 1990; Millar et al. 2000) A more recent study has also identified six unrelated schizophrenia patients with a shared NDE1 missense mutation, S214F.(Kimura et al. 2015) Intriguingly, this mutation is adjacent to the NDE1 T215

residue, which is a known target of Cdk1 and Cdk5.(Alkuraya et al. 2011; Hirohashi et al. 2006) How defects in NDE1 expression and phosphorylation might contribute to this disease is unknown.

The current study was initiated to determine the functions of Nde1 phosphorylation in the developing brain. We present the first data demonstrating a role for phosphorylation at each of three majors predicted Nde1 CDK1 sites in the developing rat neocortex, T215, T243, and T246. Importantly, these data provide clear support for a distinct, direct role for Nde1 phosphorylation in controlling the classic RGP nuclear oscillations comprising interkinetic nuclear migration. In addition, we identify a single Nde1 phosphorylation site, Nde1 T246, which *directly* controls mitotic entry. Finally, we provide evidence that Nde1 phosphorylation at a predicted CDK1 residue is affected by mutation of the adjacent schizophrenia-associated Nde1 residue, a novel experimental link between a cytoplasmic dynein regulatory gene and a neuropsychiatric disorder.

Results

Nde1 phosphomutants fail to fully rescue Nde1 shRNA effects in RGP Cells

To determine the physiological effects of Nde1 phosphorylation in brain development, we first focused on the three Cdk1 sites: T215, T243, and T246. Of these sites, T243 is also a predicted Cdk5 target. We performed *in utero* electroporation in embryonic day 16 (E16) rat embryos by injecting either GFP or Nde1 shRNA in combination with mCherry- tagged Nde1 constructs into the left cortical ventricle. Nde1 is visible in these cells as a cytoplasmic signal that can also display punctate staining. Nde1 can also be seen decorating the nuclear envelope in some cases, depending on the stage of the cell cycle. Expression of GFP or of Nde1 shRNA alone were used as controls. At E20 or postnatal day 6 (P6), brains were fixed and examined for defects in neocortical development. Apical endfoot length in the RGPs was calculated from the distance from the apical side of the nucleus to the ventricular surface of the cortex. Consistent with previous work, Nde1 shRNA resulted in accumulation of nuclei between 10 and 15μm from the ventricular surface, with results calculated as the percent of RGPs with a measured apical endfoot length (AEL) of 15 μm or less. Mitotic index was calculated as the percentage of transfected cells that were phospho-Histone H3 (PH3) positive compared to the total number of transfected cells.

As previously observed,(Doobin et al. 2016) Nde1 RNAi caused accumulation of the majority of RGP nuclei between 10 and 15μm from the ventricular surface of the developing rat brain (Figure 2A-B). Co-expression with wild-type shRNA-resistant NDE1 restored the RGP nuclei to their expected distribution relative to the VS (Figure 2A-B). The mitotic index for the Nde1 shRNA-expressing RGP cells was also markedly reduced, an effect that could be rescued by co-expression of wild-type NDE1 (Figure 2C), in agreement with the results of previously published studies.[3] We also performed Nde1 RNAi rescue with a triple phosphomutant construct (T215A, T243A, and T246A, referred to here as Nde1x3A). As the fluorophore in this and other experiments shown in Figures 2,3,4, and 6 is directly conjugated to Nde1, the signal is visible as small puncta in Figure 2Aiii'-2Aiv'''. The Nde1x3A construct failed to restore either INM or mitotic index, resulting in a distribution of RGP nuclei similar to that caused by Nde1 RNAi alone

(Figure 2A-C). Together, these results suggest that INM, and as a consequence, RGP cell proliferation, are each regulated by Nde1 phosphorylation.

To determine the relative physiological importance of individual Nde1 phosphorylation sites, the effects of single-site phosphomutant constructs were also examined. For this purpose, we co-expressed a Nde1 shRNA along with RNAi-resistant versions of Nde1:T215A or T243A. Neither construct rescued the defect in INM caused by Nde1 shRNA. Instead, these treatments resulted in the accumulation of RGP nuclei between 10 and 15μm from the ventricular surface, similar to the effect seen of Nde1x3A expression or of Nde1 knockdown alone (Figure 2A-B). The T215A and T243A mutations also resulted in a reduced mitotic index (Figure 2D). Interestingly, rescue of Nde1 RNAi with a mutation in the third site tested, T246A, resulted in accumulation of cells directly adjacent to the ventricular surface, though mitotic index was still reduced compared to the WT level (Figure 2A-C). Although all constructs tested, other than WT Nde1, showed an increase in the percent of cells with an AEL less than 15 μm, the T246A construct was the only one tested to result in an increase in the percent of cells with an AEL less than 5 μm (Figure 2C). This accumulation so close to the ventricular surface indicates that the T246A construct is able to overcome the late G2 INM stalling, seen in the other conditions tested, but is nonetheless unable to rescue mitotic index. These results suggest that Nde1-T246A can rescue INM, but fails to rescue proper mitosis, likely through arrest at the G2/M transition, as shown previously.(Alkuraya et al. 2011).This result is similar to the effects of Nde1 knockdown in combination with BicD2 rescue, where we found that BicD2 overexpression can rescue INM , though the cells remained arrested in G2 and failed to enter mitosis.[3]

We also tested for dominant negative effects of the Nde1 mutations (Figure 3). As Nde1 is dimeric, we expected that the phosphomutant form might interact with WT Nde1, resulting in a dimer that was less effective at recruiting dynein to the RGP cell nucleus. This was tested by injecting an GFP reporter along with each Nde1 construct. In two cases - T243A, and Nde1x3A - we detected clear inhibition of INM (Figure 3A-B). Expression of either the T215A or T246A Nde1 cDNA constructs showed no effect on INM or mitotic index (Figure 3B-C). The only significant effect on mitotic index we observed was in T243A- and Nde1x3A-expressing cells (Figure 3C). In these cases, mitotic index was significantly reduced compared to GFP alone. As a control, we also included WT Nde1 and GFP control, which showed no effect on INM or mitotic index (Figure 3Aiii, B-C)

Nde1 phosphomimetics fail to fully rescue Nde1 shRNA effects in RGPs

To further test the validity of our phosphorylation site mutations, we used a Nde1 construct containing mutations from T to glutamic acid at T215, T243, and T246, rather than alanine, in order to mimic the charge of a phosphorylated residue. We tested the effect of this construct (Nde1x3E) on both INM and mitotic index. We found that Nde1x3E had no effect on INM, either when co-transfected with Nde1 shRNA, or GFP control (Figure 4B). This indicates that the phosphomimetic Nde1 is able to rescue Nde1 function in INM, and that it exhibits no dominant negative effect in the presence of endogenous Nde1. The mitotic index results, however, showed no effect in the GFP control and Nde1x3E conditions, but did show a significant decrease in mitotic index when Nde1x3E was co-transfected with Nde1 shRNA (Figure 4C). This was an unexpected result, as all phosphomutants expressed in combination with Nde1

shRNA resulted in a decrease in mitotic index. Only the T243A and Nde1x3A constructs had a dominant effect on mitotic index without Nde1 shRNA present. This observation may indicate that the three sites must be phosphorylated in a specific combination in order to trigger mitotic entry, and one or more sites must be dephosphorylated in order for this to occur.

Expression of NDE1 mutated at residues T215 or T243 showed results consistent with an inability to effectively recruit dynein to the nuclear envelope during INM, with T243A construct causing a dominant negative effect. We note that expressing the Nde1 T246A displayed an unexpected phenotype: persistence of functional INM but a reduction in mitotic index. Therefore, we next tested a T246 phosphomimetic construct, T246E, (Figure 4D-G. T246E in combination with Nde1 shRNA failed to rescue INM (Figure 4E), indicating that T246 must be *dephosphorylated* in order to effectively function in INM. When endogenous Nde1 is present, as in the GFP + T246E condition, INM is rescued, as this condition shows not only an increase in the percent of cells with an AEL less than 15 μm (Figure 4F), but also an increase in the percent of cells less than 5 μm from the ventricular surface (Figure 4G), similar to the results from the Nde1 shRNA + T246A condition. Interestingly, RGP cells expressing T246E also fail to progress through mitosis, even in the presence of endogenous WT Nde1 (Figure 4G). As Nde1 has multiple roles throughout the cell cycle it is possible that the two constructs arrest mitotic progression at different stages, but with the same effect of reducing overall mitotic index. T246A has already been shown to arrest cells in the G2/M transition,(Alkuraya et al. 2011) and a Nde1 interaction with CENP-F may be artificially stabilized by the T246E mutation, 'tethering' dynein to kinetochores and preventing the stripping of spindle assembly checkpoint (SAC) proteins from the cytoskeleton, and therefore interfering with mitotic progression.(Auckland et al., n.d.) It is also possible that another kinase, Aurora A for example, is responsible for the mitotic phosphorylation of Nde1, as it is for Ndel1 HeLa cells.(Mori et al. 2007)

A schizophrenia-associated Nde1 mutation affects post-mitotic neuronal development, but not RGP cell behavior

A missense mutation in NDE1, S214F, has been reported to be associated with a form of schizophrenia in a cohort of six unrelated Japanese patients.(Kimura et al. 2015) Nde1-S214 has been neither shown nor predicted to be phosphorylated. Nonetheless, to account for its particular pathophysiological effects, the S214F mutation was postulated to act in a highly unusual manner, sterically hindering phosphorylation of the adjacent T215 residue.[22] To test this hypothesis we performed direct *in vitro* phosphorylation of recombinant NDE1 using commercially available CDK5.

We note that the S214F schizophrenia mutation replaces a polar hydrophilic amino acid with an aromatic, very hydrophobic one, which has a bulky side chain that might have a marked effect on the local 3D structure of the polypeptide. We hypothesized that this conformational perturbation may affect Cdk5 accessibility to the adjacent T215 site, thereby reducing the ability of the protein kinase to phosphorylate Nde1. Because Cdk5 is also predicted to phosphorylate T243 and T246, we mutated these two residues from T to A before expressing and purifying GST-Nde1, with or without the S214F mutation (referred to as S214F-T243A-T246A and T243A-T246A). This was done to ensure that the effect on phosphorylation was limited to T215. We then performed an *in vitro* kinase assay with recombinant Cdk5 and detected a 90% decrease in Nde1 phosphorylation in the NDE1 S214F schizophrenia mutation. Phosphorylation was assessed by quantitative immunoblotting of the recombinant Nde1-expressing cells using an

anti-phospho-threonine antibody (Figure 4A, C). We also found the presence of Nde1-S214F to cause a small, but non-significant, decrease in the level of Nde1 phosphorylation by Cdk1 (Figure 4A-B). These results suggest therefore, that mutation of the Nde1 S214 residue inhibits Cdk5, but not Cdk1, phosphorylation at T215. Though Cdk1 phosphorylation is slightly (though not significantly reduced, the ratio of phospho-Nde1:total Nde1, even with S214F, is higher for Cdk1 than for Cdk5. This may explain why the S214F mutation appears to affect Cdk5 phosphorylation more so than it inhibits Cdk1. If Cdk5 is more sensitive than Cdk1 to steric hinderance in the S214F mutant Nde1, this would agree with our *in vivo* results, wherein we see no effect of S214F on Nde1 function in RGP cells, where we expect Cdk1 to have a predominant role and Cdk5 is not expressed.

To test the effects of the specific inhibition of Cdk5phosphorylation in S214F constructs, GFP was co-transfected with mCherry tagged Nde1-S214F in E16 rat brains (Figure 6). As all six known patients with the S214F mutation are heterozygous for this mutation, we did not perform concurrent knockdown of Nde1 with expression of the S214F mutation. Electroporation with Nde1-S214F cDNA had no effect on the distribution of RGP nuclei relative to the VS, or on RGP mitotic index by E20 (Figure 6B-C). As Cdk5 is preferentially expressed in post-mitotic neurons,[27] and not in RGPs, this result is consistent with the *in vitro* kinase assay. If Cdk1 phosphorylation of Nde1 was affected by the S214F mutation, we might expect to see altered INM and mitotic entry in RGPs, but as Cdk5 phosphorylation appears to be specifically inhibited, we might expect to see results only in cells that express Cdk5.

Given that Cdk5 is preferentially expressed in post-mitotic neurons,(Smith, Greer, and Tsai 2001) we next investigated whether the S214F mutation might selectively impair post-mitotic neuronal migration. To test this possibility, we performed *in utero* electroporation with a cDNA encoding Nde1-S214F in a construct containing an IRES sequence and RFP. In these experiments, Nde1 is not directly tagged, and the RFP signal is diffuse throughout the cell. This was done so the RFP signal would fill the cell, in order to visualize its entire morphology. In addition to a lack of effect on INM, The S214F mutation had no detectable effect on neuronal migration to the cortical plate at E20 (Figure 7A-B). Impaired neuronal migration at E20 might be expected from inhibition of Cdk5 phosphorylation if Nde1 recruitment to the neuronal NE is altered, preventing the cell body from translocating. Importantly, this mutation did alter the morphology of the leading process in in Nde1-S214F-expressing neurons, which showed a significant increase in the percent of cells with branched leading processes, as opposed to a single leading process. This result was also observed following Nde1-T215A expression (Figure 6C-D). We also measured the length of the leading processes in these brains (Figure 7E). Overexpression of Nde1 resulted in an increase in the overall leading process length compared to RFP alone, and both T215A and S214F constructs showed significantly reduced leading process length compared to cells expressing WT Nde1 (Figure 7E). As the two mutations, T215A and S214 F, result in a similar phenotype in E20 neurons, the likely explanation is that they both affect Cdk5 phosphorylation at T215, altering the morphology of leading processes. The T215A mutation prevents this by altering the phosphorylated residue, while S214F prevents T215 phosphorylation by blocking Cdk5 phosphorylation of the adjacent T215, likely through steric hinderance.

In order to observe more long-term effects of the S214F mutation, we examined postnatal day 6 (P6) neocortical rat brain slices. The results further supported a neuronal migration defect. Our fixed cell analysis also revealed a clear reduction in neuronal number in layers 2/3 of the developing neocortex, as judged using Cux1 staining (Figure 8A-B). WT Nde1 overexpression resulted in a significantly higher percent of cells below layer 2/3 compared to RFP alone, while the T215A and S214F constructs showed a significant reduction in cells below layer 2/3 compared to WT Nde1 (Figure 8B). In contrast, Nde1 KD at P6 results in cells that accumulate primarily within the white matter (Figure 8C) and display proliferative markers that are never seen in the other conditions at P6 (Figure 8D-F).

Discussion

Considerable progress has been made in understanding the physiological roles of Nde1 and Ndel1 in neocortical development. There is strong evidence for a Nde1 contribution to INM, as well as to post-mitotic neuronal migration.(Doobin et al. 2016) We have now tested the role of three Nde1 phosphorylation sites in rat brain development. We observed clear and potent effects of specific Nde1 phosphorylation-state mutations in the control of INM. Our results also provide strong support for new insight into the little-understood mechanism we uncovered for triggering RGP mitotic entry.(Doobin et al. 2016) Finally, in the course of these studies we obtained clear evidence for a novel post-mitotic role for Nde1 phosphorylation in schizophrenia.

Differential Roles of Nde1 phosphorylation sites in INM vs. Mitotic entry

Our data serve to validate predicted CDK1 phosphorylation sites at Nde1 residues T215, T243, and T246. We previously evaluated these sites for a role in mitosis in nonneuronal cells and found them to be required for Nde1 binding to the G2 nuclear envelope (NE) as and to prometaphase-to-early anaphase kinetochores in HeLa cells.(Wynne and Vallee 2018) *In vitro* analysis performed in that study further revealed that Nde1 phosphorylation enhances its physical interaction with CENP-F, which showed a similar, if not identical, distribution to that of Nde1 in mitotic Hela cells. Here we find a requirement for the same trio of Nde1 sites in RGP mitotic entry in RGP cells. Our current data further indicate that mutations at Nde1 residues T215 and T243 specifically interfere with apical INM in RGPs, presumably due to a failure in recruitment of Nde1 and, in turn, cytoplasmic dynein, to the NE during G2. Given that the T215A and T243A mutations each fail to rescue INM in Nde1 shRNA-expressing RGPs, it is likely that both sites must be phosphorylated in order for INM to proceed. We speculate that this might help ensure that mitotic entry cannot occur until RGP cells are sufficiently far along in G2 progression and apical INM.

We find that another Nde1 phosphorylation site, T246, has a novel and distinct function: mutation of this site alone is sufficient to block mitosis without affecting apical INM. It is possible that the T215 and T243 sites must also be phosphorylated for mitotic entry to occur. However, we were unable to test the role of these sites in mitotic entry directly, as their phosphomutant forms arrested cells earlier in G2, during apical INM. Rescue of Nde1 knockdown with the phosphomutant T246A resulted, however, in complete INM, and arrest of RGP nuclei prior to mitotic entry. We do not yet know the specific role of Nde1 in this unexpected mitotic entry

control behavior. However, attention to the T246 phosphorylation site may provide yet further insight into mitotic entry requirements of RGPs beyond simple completion of apical INM. A triple phosphomimetic Nde1 construct is able to rescue INM, but not mitotic entry, under Nde1 KD conditions. This indicates that there may be a specific combination of phosphorylation required for effective progress through INM and mitosis. These results are modeled in Figure 9. An important note is that, in our system, constructs that fail to rescue INM will also fail to rescue mitotic index, as the arrested cells cannot reach the ventricular surface to divide, and we cannot be sure whether these residues have a direct or indirect role in mitotic entry.
We note further that our results appear to resolve a long-standing question, the regulation of the mysterious nuclear oscillatory behavior that constitutes INM. Further work will be needed to understand the full physiological function of this behavior.

A role for Nde1 in schizophrenia

Recent genetic studies have implicated one of the Nde1 phosphorylation sites, Nde1-T215, in schizophrenia. A heterozygous mutation, Nde1 S214F, was found in six unrelated patients with the disease.(Kimura et al. 2015) This residue is not, itself, phosphorylated by CDK1 or CDK5, but was proposed to interfere sterically with the ability of CDK1 or CDK5 to phosphorylate the adjacent T215 residue. We tested this interesting hypothesis directly, and found it, to be valid: phosphorylation of Nde1 by CDK5 was, indeed, inhibited by the S214F mutation, most likely through steric hinderance of CDK5 phosphorylation at Nde1-T215. Interestingly, CDK1 phosphorylation was largely unaffected. This kinase specificity of T215 seems to be of clear relevance in resolving the molecular basis for the S214F phenotype. In addition to their implications for this particular schizophrenia mechanism, these results indicate how critical phosphoregulation of Nde1 is, and at multiple stages of brain development.

Another important feature of S214F is the nature of the brain developmental phenotype we observe. Unlike the three NDE1 phosphorylation sites we examined, S214F appears to affect post-mitotic aspects of neocortical development in particular. This is consistent with Cdk5 expression in post-mitotic neurons, but not RGPs. We further observed abnormal lamination of Nde1-S214F-expressing cells in the developing neocortex, an unusual, if not unique, anatomic effect of the S214F mutation. This abnormality is similar to the delayed cortical lamination observed in models of Fragile-X syndrome.(Lee et al. 2019) We speculate that Improper neocortical layering might contribute to synaptic abnormalities, which could predispose patients to neuropsychiatric disease. Further investigation of the long-term effects of abnormal neocortical lamination on synaptic development and adult neocortical function will be required to resolve the full effects of the of the S214F mutation and its developmental consequences.

Materials and Methods

In utero electroporation. Plasmids were transfected by intraventricular injection into the left ventricle of rats at embryonic day 16 (E16) and electroporating the embryos by using a tweezer electrode on either side of the skull outside the external wall of the uterine horn, with the positive electrode adjacent to the injected ventricle. All animal protocols were approved by the Institutional Animal Care and Use Committee at Columbia University.

Cortical slice preparation and immunostaining. 4 days following the in-utero electroporation procedures, the embryos were dissected from the uterus. Embryonic brains were dissected and fixed in 4% paraformaldehyde in PBS for 24 hours at 4°C. Following fixation, the brains were embedded in 4% agarose in PBS and sliced by a vibratome (Zeiss) in 100mm thick coronal sections. The sections were incubated in blocking solution containing PBS with 0.3% Triton X-100 and 5% normal donkey serum for 1 h. Brains were incubated with primary antibodies overnight in blocking solution at 4°C, then sections were washed 3 times in PBS, and incubated in secondary antibodies in blocking solution for 2 h at room temperature. The sections were mounted on slides using Aqua-Poly/Mount (Polysciences, Inc).

RNAi and DNA constructs. An shRNA construct was designed to target NDE1 and cloned into a pRetro-U6G vector (Cellogenetics, MD, USA), which co-expressed GFP and the shRNA target sequences. The target sequence for NDE1 is 50-GCGTTTGAATCAAGCCAT TGA-30. Empty vectors of pEGFP-C1 and pmCherry-N1 were used as controls (Clontech). For overexpression of NDE1, mouse cDNA for Nde1 was cloned into a mCherry fluorescent reporter (mCherry-C1-NDE1) and subcloned into a pCAGEN vector driven by CAG promoter (provided by Connie Cepko (Addgene plasmid #11160)) using XhoI and NotI restriction sites. Five silent point mutations were made using KOD Hot Start (Millipore) to introduce shRNA resistance in the construct.

Antibodies. Antibodies used in this study were mouse monoclonal against phosphohistone H3 (Abcam, ab14955, 1:500 dilution), Pax6 (Covance, PRB-278p, 1:300 dilution) S100ß (Millipore, 04-1054, 1:300 dilution), and Ki67 (Millipore, MAB4190, 1:250 dilution). Antibodies were used together with DAPI (4',6-diamidino-2-phenylindole, Thermo Scientific, 62248, 1:1,000 dilution). NDE1 (Abnova, H00054820-M01, 1:1,000 dilution) and a-tubulin (Sigma; 1:2,000) were used for immunoblotting. To develop in a LICOR system, fluorescent secondary antibodies were acquired from Invitrogen (dilution 1:10,000) and Rockland (dilution 1:10,000) to use for western blotting.

Imaging and statistical analysis. All images were collected with an IX80 laser scanning confocal microscope (Olympus FV100 Spectral Confocal System). Brain sections were imaged using a 60X 1.42 N.A. oil objective or a 10X 0.40 N.A. air objective. All images were analyzed using ImageJ software (NIH, Bethesda, MD, USA). Apical process length and mitotic index measurements were also performed using this software. All statistical analysis was performed using Prism (GraphPad Software, La Jolla, CA, USA) or R. For all analyses, significance was accepted at the level of $P<0.05$. All brain measurements were made from at least three different embryonic rat brains across at least two mothers. Animals from all successful operations were included in the analysis. At least two conditions were used in each pregnant mother, depending on litter size. The constructs injected into each embryo must be carefully noted in order to keep track of the embryo from surgery to data analysis, so the investigators were not blinded, but images were independently analyzed by multiple investigators to ensure that results were consistent.

Protein purification. Mouse Nde1 cDNA was cloned into the pGEX 6.1 vector using BamHI/NotI sites. Residues Threonine 243 and Threonine 246 were mutagenized into Alanine with KOD polymerase (T243A-T246A). Next, residue Serine 214 was mutated to Phenylalanine with KOD polymerase (S214F). GST-Nde1-T243A-T246A and GST-Nde1-S214F-T243A-T246A constructs were expressed in Rosetta BL21 cells with 0.1mM IPTG at 19°C overnight and purified with GSH beads. 200 ml cultures were lysed in 500 mM NaCl, 50 mM Tris-HCl pH 7.5, 1mM DTT, complete EDTA-free protease inhibitors, 1mM lysozyme, and bound to 600 ul slurry of GSH agarose beads (brand) for 2 h. After 3 washes in 10 bed volumes of 300 mM NaCl, 50 mM Tris-HCl pH 7.5, 1mM DTT, the GST-tagged protein was eluted in 250 mM NaCl, 50 mM Tris-HCl pH 7.5, 1mM DTT, 20 mM reduced GSH, and dialyzed overnight against 150 mM NaCl, 50 mM Tris-HCl pH 7.5, 1mM DTT.

Kinase assay. 10 ug of GST-Nde1-T243A-T246A or GST-Nde1-S214F-T243A-T246A were incubated with or without 0.2 ug active Cdk5 or Cdk1 (Millipore), 400 uM ATP, 10x PK buffer for 45 min at 30C. The kinase reaction was stopped by adding Llaemli loading buffer. A volume of the reaction corresponding to ~1 ug of GST-tagged protein was loaded on SDS-PAGE gel for western blot analysis. Antibodies used: anti phosphor-Thr(Pro) (Cell Signaling, 1:1000), anti Nde1 (generated as in Stehman et al., 2007)(Stehman et al. 2007), anti Cdk5 (Santa Cruz, 1: 5000).

Acknowledgments

The authors thank the members of the Vallee lab for helpful discussions.

References

Alkuraya, Fowzan S., Xuyu Cai, Carina Emery, Ganeshwaran H. Mochida, Mohammed S. Al-Dosari, Jillian M. Felie, R. Sean Hill, et al. 2011. “Human Mutations in NDE1 Cause Extreme Microcephaly with Lissencephaly.” *American Journal of Human Genetics* 88 (5): 536–47. https://doi.org/10.1016/j.ajhg.2011.04.003.

Auckland, Philip, Emanuele Roscioli, Helena Louise Elvidge Coker, and Andrew D. McAinsh. n.d. “CENP-F Stabilizes Kinetochore-Microtubule Attachments and Limits Dynein Stripping of Corona Cargoes.” Accessed June 27, 2024. https://doi.org/10.1083/jcb.201905018.

Baffet, Alexandre D., Daniel J. Hu, and Richard B. Vallee. 2015. “Cdk1 Activates Pre-Mitotic Nuclear Envelope Dynein Recruitment and Apical Nuclear Migration in Neural Stem Cells.” *Developmental Cell* 33 (6): 703–16. https://doi.org/10.1016/j.devcel.2015.04.022.

Bakircioglu, Mehmet, Ofélia P. Carvalho, Maryam Khurshid, James J. Cox, Beyhan Tuysuz, Tanyeri Barak, Saliha Yilmaz, et al. 2011. “The Essential Role of Centrosomal NDE1 in Human Cerebral Cortex Neurogenesis.” *American Journal of Human Genetics* 88 (5): 523–35. https://doi.org/10.1016/j.ajhg.2011.03.019.

Blackwood, D. H. R., A. Fordyce, M. T. Walker, D. M. St. Clair, D. J. Porteous, and W. J. Muir. 2001. “Schizophrenia and Affective Disorders—Cosegregation with a Translocation at Chromosome 1q42 That Directly Disrupts Brain-Expressed Genes: Clinical and P300 Findings in a Family.” *American Journal of Human Genetics* 69 (2): 428–33.

Bolhy, Stéphanie, Imène Bouhlel, Elisa Dultz, Tania Nayak, Michela Zuccolo, Xavier Gatti, Richard Vallee, Jan Ellenberg, and Valérie Doye. 2011. “A Nup133-Dependent NPC-

Anchored Network Tethers Centrosomes to the Nuclear Envelope in Prophase." *Journal of Cell Biology* 192 (5): 855–71. https://doi.org/10.1083/jcb.201007118.
Doobin, David J., Shahrnaz Kemal, Tiago J. Dantas, and Richard B. Vallee. 2016. "Severe *NDE1*-Mediated Microcephaly Results from Neural Progenitor Cell Cycle Arrests at Multiple Specific Stages." *Nature Communications* 7 (August):12551. https://doi.org/10.1038/ncomms12551.
Feng, Yuanyi, Eric C. Olson, P. Todd Stukenberg, Lisa A. Flanagan, Marc W. Kirschner, and Christopher A. Walsh. 2000. "LIS1 Regulates CNS Lamination by Interacting with mNudE, a Central Component of the Centrosome." *Neuron* 28 (3): 665–79. https://doi.org/10.1016/S0896-6273(00)00145-8.
Hebbar, Sachin, Mariano T. Mesngon, Aimee M. Guillotte, Bhavim Desai, Ramses Ayala, and Deanna S. Smith. 2008. "Lis1 and Ndel1 Influence the Timing of Nuclear Envelope Breakdown in Neural Stem Cells." *The Journal of Cell Biology* 182 (6): 1063–71. https://doi.org/10.1083/jcb.200803071.
Hirohashi, Y., Q. Wang, Q. Liu, B. Li, X. Du, H. Zhang, K. Furuuchi, K. Masuda, N. Sato, and M. I. Greene. 2006. "Centrosomal Proteins Nde1 and Su48 Form a Complex Regulated by Phosphorylation." *Oncogene* 25 (45): 6048–55. https://doi.org/10.1038/sj.onc.1209637.
Hirotsune, S., M. W. Fleck, M. J. Gambello, G. J. Bix, A. Chen, G. D. Clark, D. H. Ledbetter, C. J. McBain, and A. Wynshaw-Boris. 1998. "Graded Reduction of Pafah1b1 (Lis1) Activity Results in Neuronal Migration Defects and Early Embryonic Lethality." *Nature Genetics* 19 (4): 333–39. https://doi.org/10.1038/1221.
Hu, Daniel Jun-Kit, Alexandre Dominique Baffet, Tania Nayak, Anna Akhmanova, Valérie Doye, and Richard Bert Vallee. 2013. "Dynein Recruitment to Nuclear Pores Activates Apical Nuclear Migration and Mitotic Entry in Brain Progenitor Cells." *Cell* 154 (6): 1300–1313. https://doi.org/10.1016/j.cell.2013.08.024.
Johnstone, Mandy, Alan Maclean, Lien Heyrman, An-Sofie Lenaerts, Annelie Nordin, Lars-Göran Nilsson, Peter De Rijk, et al. 2015. "Copy Number Variations in DISC1 and DISC1-Interacting Partners in Major Mental Illness." *Molecular Neuropsychiatry* 1 (3): 175–90. https://doi.org/10.1159/000438788.
Jumper, John, Richard Evans, Alexander Pritzel, Tim Green, Michael Figurnov, Olaf Ronneberger, Kathryn Tunyasuvunakool, et al. 2021. "Highly Accurate Protein Structure Prediction with AlphaFold." *Nature* 596 (7873): 583–89. https://doi.org/10.1038/s41586-021-03819-2.
Kimura, Hiroki, Daisuke Tsuboi, Chenyao Wang, Itaru Kushima, Takayoshi Koide, Masashi Ikeda, Yoshimi Iwayama, et al. 2015. "Identification of Rare, Single-Nucleotide Mutations in NDE1 and Their Contributions to Schizophrenia Susceptibility." *Schizophrenia Bulletin* 41 (3): 744–53. https://doi.org/10.1093/schbul/sbu147.
Klinman, Eva, Mariko Tokito, and Erika L. F. Holzbaur. 2017. "CDK5-Dependent Activation of Dynein in the Axon Initial Segment Regulates Polarized Cargo Transport in Neurons." *Traffic (Copenhagen, Denmark)* 18 (12): 808–24. https://doi.org/10.1111/tra.12529.
Kriegstein, Arnold, and Arturo Alvarez-Buylla. 2009. "The Glial Nature of Embryonic and Adult Neural Stem Cells." *Annual Review of Neuroscience* 32 (1): 149–84. https://doi.org/10.1146/annurev.neuro.051508.135600.
Lee, Frankie H. F., Terence K. Y. Lai, Ping Su, and Fang Liu. 2019. "Altered Cortical Cytoarchitecture in the Fmr1 Knockout Mouse." *Molecular Brain* 12 (June):56. https://doi.org/10.1186/s13041-019-0478-8.
Millar, J. K., J. C. Wilson-Annan, S. Anderson, S. Christie, M. S. Taylor, C. A. Semple, R. S. Devon, et al. 2000. "Disruption of Two Novel Genes by a Translocation Co-Segregating

with Schizophrenia." *Human Molecular Genetics* 9 (9): 1415–23. https://doi.org/10.1093/hmg/9.9.1415.
Mori, Daisuke, Yoshihisa Yano, Kazuhito Toyo-oka, Noriyuki Yoshida, Masami Yamada, Masami Muramatsu, Dongwei Zhang, et al. 2007. "NDEL1 Phosphorylation by Aurora-A Kinase Is Essential for Centrosomal Maturation, Separation, and TACC3 Recruitment." *Molecular and Cellular Biology* 27 (1): 352–67. https://doi.org/10.1128/MCB.00878-06.
Ozeki, Yuji, Toshifumi Tomoda, John Kleiderlein, Atsushi Kamiya, Lyuda Bord, Kumiko Fujii, Masako Okawa, et al. 2003. "Disrupted-in-Schizophrenia-1 (DISC-1): Mutant Truncation Prevents Binding to NudE-like (NUDEL) and Inhibits Neurite Outgrowth." *Proceedings of the National Academy of Sciences* 100 (1): 289–94. https://doi.org/10.1073/pnas.0136913100.
Pandey, Jai P., and Deanna S. Smith. 2011. "A Cdk5-Dependent Switch Regulates Lis1/Ndel1/Dynein-Driven Organelle Transport in Adult Axons." *The Journal of Neuroscience: The Official Journal of the Society for Neuroscience* 31 (47): 17207–19. https://doi.org/10.1523/JNEUROSCI.4108-11.2011.
Pawlisz, Ashley S., Christopher Mutch, Anthony Wynshaw-Boris, Anjen Chenn, Christopher A. Walsh, and Yuanyi Feng. 2008. "Lis1–Nde1-Dependent Neuronal Fate Control Determines Cerebral Cortical Size and Lamination." *Human Molecular Genetics* 17 (16): 2441–55. https://doi.org/10.1093/hmg/ddn144.
Reiner, O., R. Carrozzo, Y. Shen, M. Wehnert, F. Faustinella, W. B. Dobyns, C. T. Caskey, and D. H. Ledbetter. 1993. "Isolation of a Miller-Dieker Lissencephaly Gene Containing G Protein Beta-Subunit-like Repeats." *Nature* 364 (6439): 717–21. https://doi.org/10.1038/364717a0.
Smith, D. S., P. L. Greer, and L. H. Tsai. 2001. "Cdk5 on the Brain." *Cell Growth & Differentiation: The Molecular Biology Journal of the American Association for Cancer Research* 12 (6): 277–83.
Splinter, Daniël, David S. Razafsky, Max A. Schlager, Andrea Serra-Marques, Ilya Grigoriev, Jeroen Demmers, Nanda Keijzer, et al. 2012. "BICD2, Dynactin, and LIS1 Cooperate in Regulating Dynein Recruitment to Cellular Structures." *Molecular Biology of the Cell* 23 (21): 4226–41. https://doi.org/10.1091/mbc.E12-03-0210.
Splinter, Daniël, Marvin E. Tanenbaum, Arne Lindqvist, Dick Jaarsma, Annette Flotho, Ka Lou Yu, Ilya Grigoriev, et al. 2010. "Bicaudal D2, Dynein, and Kinesin-1 Associate with Nuclear Pore Complexes and Regulate Centrosome and Nuclear Positioning during Mitotic Entry." *PLOS Biology* 8 (4): e1000350. https://doi.org/10.1371/journal.pbio.1000350.
St Clair, D., D. Blackwood, W. Muir, M. Walker, D. St Clair, W. Muir, A. Carothers, G. Spowart, C. Gosden, and H. J. Evans. 1990. "Association within a Family of a Balanced Autosomal Translocation with Major Mental Illness." *The Lancet* 336 (8706): 13–16. https://doi.org/10.1016/0140-6736(90)91520-K.
Stehman, Stephanie A., Yu Chen, Richard J. McKenney, and Richard B. Vallee. 2007. "NudE and NudEL Are Required for Mitotic Progression and Are Involved in Dynein Recruitment to Kinetochores." *The Journal of Cell Biology* 178 (4): 583–94. https://doi.org/10.1083/jcb.200610112.
Strzyz, Paulina J., Hyun O. Lee, Jaydeep Sidhaye, Isabell P. Weber, Louis C. Leung, and Caren Norden. 2015. "Interkinetic Nuclear Migration Is Centrosome Independent and Ensures Apical Cell Division to Maintain Tissue Integrity." *Developmental Cell* 32 (2): 203–19. https://doi.org/10.1016/j.devcel.2014.12.001.

Toyo-oka, Kazuhito, Aki Shionoya, Michael J. Gambello, Carlos Cardoso, Richard Leventer, Heather L. Ward, Ramses Ayala, et al. 2003. “14-3-3ε Is Important for Neuronal Migration by Binding to NUDEL: A Molecular Explanation for Miller–Dieker Syndrome.” *Nature Genetics* 34 (3): 274–85. https://doi.org/10.1038/ng1169.

Tsai, Jin-Wu, Wei-Nan Lian, Shahrnaz Kemal, Arnold Kriegstein, and Richard B. Vallee. 2010. “An Unconventional Kinesin and Cytoplasmic Dynein Are Responsible for Interkinetic Nuclear Migration in Neural Stem Cells.” *Nature Neuroscience* 13 (12): 1463–71. https://doi.org/10.1038/nn.2665.

Varadi, Mihaly, Damian Bertoni, Paulyna Magana, Urmila Paramval, Ivanna Pidruchna, Malarvizhi Radhakrishnan, Maxim Tsenkov, et al. 2024. “AlphaFold Protein Structure Database in 2024: Providing Structure Coverage for over 214 Million Protein Sequences.” *Nucleic Acids Research* 52 (D1): D368–75. https://doi.org/10.1093/nar/gkad1011.

Vergnolle, Maïlys A. S., and Stephen S. Taylor. 2007. “Cenp-F Links Kinetochores to Ndel1/Nde1/Lis1/Dynein Microtubule Motor Complexes.” *Current Biology* 17 (13): 1173–79. https://doi.org/10.1016/j.cub.2007.05.077.

Wynne, Caitlin L., and Richard B. Vallee. 2018. “Cdk1 Phosphorylation of the Dynein Adapter Nde1 Controls Cargo Binding from G2 to Anaphase.” *J Cell Biol*, June, jcb.201707081. https://doi.org/10.1083/jcb.201707081.

Wynshaw-Boris, Anthony, Tiziano Pramparo, Yong Ha Youn, and Shinji Hirotsune. 2010. “Lissencephaly: Mechanistic Insights from Animal Models and Potential Therapeutic Strategies.” *Seminars in Cell & Developmental Biology* 21 (8): 823–30. https://doi.org/10.1016/j.semcdb.2010.07.008.

Żyłkiewicz, Eliza, Monika Kijańska, Won-Chan Choi, Urszula Derewenda, Zygmunt S. Derewenda, and P. Todd Stukenberg. 2011. “The N-Terminal Coiled-Coil of Ndel1 Is a Regulated Scaffold That Recruits LIS1 to Dynein.” *Journal of Cell Biology* 192 (3): 433–45. https://doi.org/10.1083/jcb.201011142.

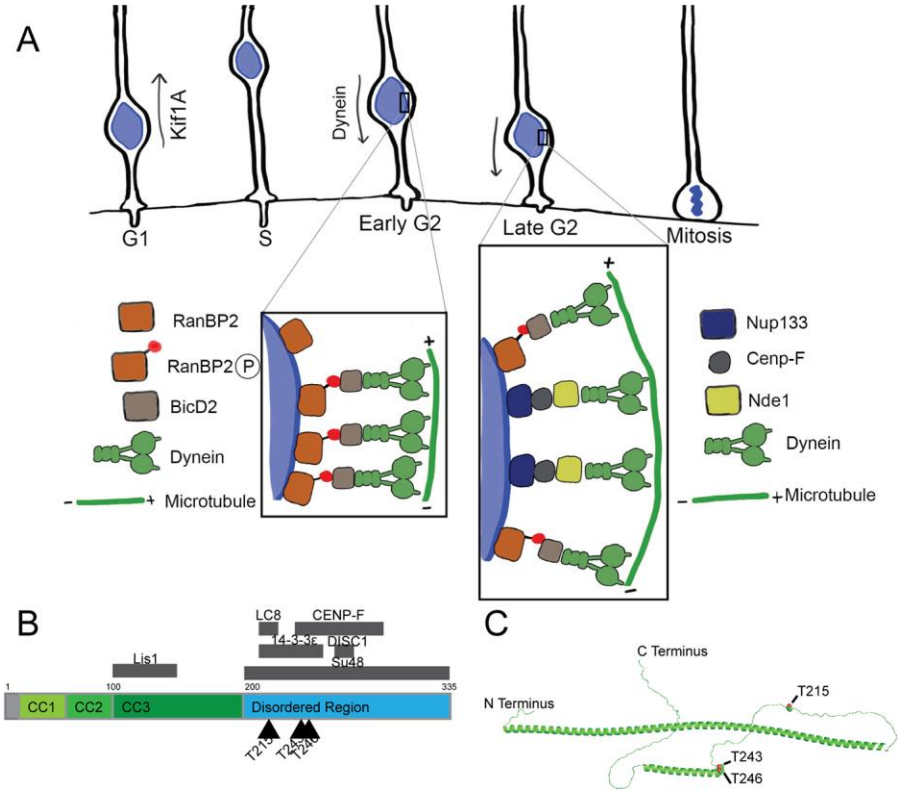

Figure 1. Schematic Representation of Nde1 roles in Neocortical Development
1A) Our previous work found Nde1 to be involved in two aspects of INM: G2-dependent apical nuclear migration and mitotic entry at the ventricular surface of the brain. Apical INM is under the control of the kinesin Kif1A and basal INM is under Dynein control. Dynein is recruited to the nuclear envelope (NE) in two stages: in early G2, phosphorylated RanBP2 bind BicD2, which binds Dynein to the NE, while in late G2, a scaffold of Nup133-CENP-F-Nde1 recruits Dynein. Once the nucleus reaches the ventricular surface, mitosis occurs. The mechanisms by which Nde1 functions in both INM and in mitotic entry are unknown. 1B) Schematic of Nde1 with Coiled Coil regions (CC1 – CC3) in green and disordered region in blue. Arrowheads indicate the location of T215, T243, and T246. Gray bars indicate binding regions in Nde1 for Lis1,(Żyłkiewicz et al. 2011) dynein (LC8),(Stehman et al. 2007) CENP-F,(Vergnolle and Taylor 2007) 14-3-3ε,(Toyo-oka et al. 2003) DISC1,(Ozeki et al. 2003) and Su48.(Hirohashi et al. 2006) Adapted from Wynne and Vallee, 2018. 1C) Predicted protein structure of Nde1 from AlphaFold,(Jumper et al. 2021; Varadi et al. 2024) with locations of T215, T243, and T246 indicated.

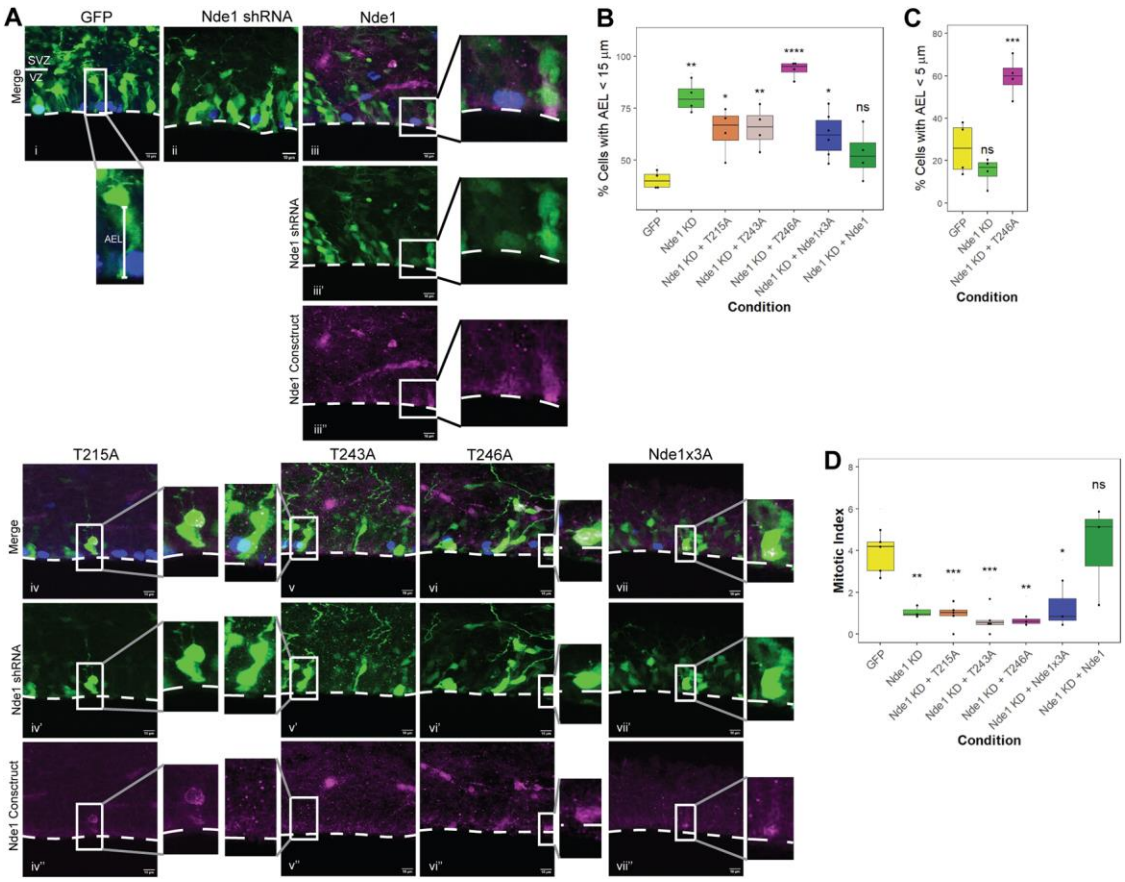

Figure 2. Rescue of Nde1 KD with Phosphomutant Constructs
2A) Representative images of RGP cells in embryonic rat brain subjected to IUE with GFP (i), Nde1 KD (ii), Nde1 KD rescued with WT Nde1 (iii); and Nde1 KD rescued with single site phosphomutants T215A (iv), T243A (v), T246A (vi), and triple phosphomutant (vii). In merged images (2Ai-vii), PH3 is shown in blue, GFP or Nde1 shRNA in green, and mCherry tagged Nde1 constructs in magenta. Nde1 shRNA is shown alone in 2Aiii'-vii'. Nde1 constructs are shown in magenta in 2Aiii''-vii'', with example cells expanded adjacent to the full images. Scale bars for all images are 10µm. A white line in the GFP control image shows the border between the SVZ (above) and VZ (below). The inset shows the measurement of apical endfoot length, from the apical end of the nucleus to the point of contact with the ventricular surface, depicted by a dashed white line in all images. 2B) Comparison of percent of cells with an apical endfoot length (AEL) less than 15 µm in RGPs expressing Nde1 shRNA and phosphomutant forms of Nde1. Apical endfoot length (AEL) was measured from the apical base of the nucleus directly to the ventricular surface in each case. 2C) Comparison of percent of cells with an apical endfoot length (AEL) less than 5 µm in RGPs expressing GFP, Nde1 shRNA, and Nde1 shRNA with T246A. 2D) Mitotic index values determined for RGP cells expressing phosphomutants of Nde1 co-transfected with Nde1 shRNA. Mitotic index was determined as the percent of transfected cells within the VZ that were positive for PH3. All statistical comparisons are made to control data. One-way ANOVA and post hoc Dunnet test were used in 2B-C, ns = not significant, *p<0.05, **p<0.01, ***p<0.001, ****p<0.0001. n = mean of values across at least 3 different

embryos from at least 2 different operations per condition. All experiments were done with E16 operations and E20 analysis in developing rat brains. 2B-C data plotted as interquartile range with 5-95% whisker range.

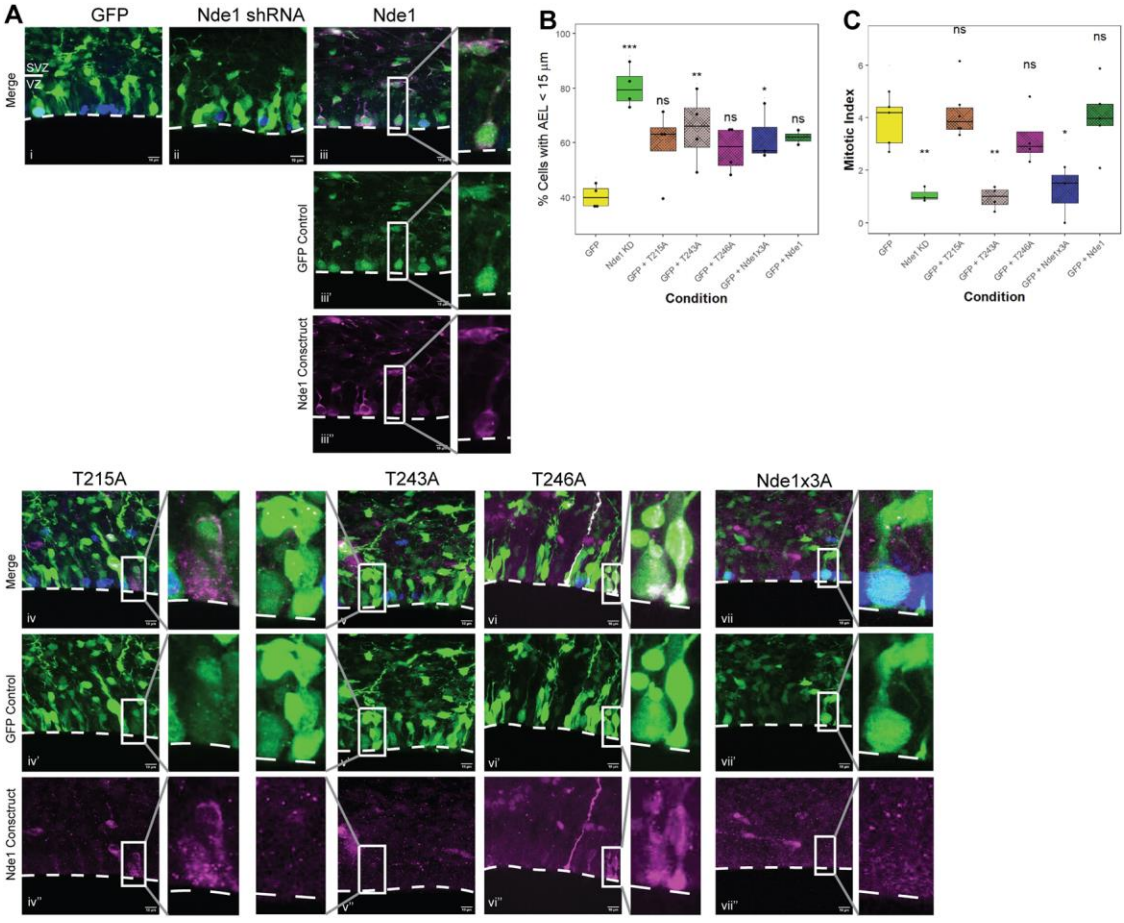

Figure 3. Dominant Negative Effects of Nde1 Phosphomutant cDNA
3A) Representative images of RGP cells in embryonic rat brain subjected to IUE with GFP control plasmid alone (i), Nde1 KD alone (ii), or GFP co-transfected with cDNAs expressing the Nde1 phosphomutants T215A (iii), T243A (iv), T246A (v) and Nde1x3A (vi). In merged images (3Ai-vii), PH3 is shown in blue, GFP or Nde1 shRNA in green, and mCherry tagged Nde1 constructs in magenta. Nde1 shRNA is shown in magenta in 3Aiii'-vii', with example cells expanded adjacent to the full images. Scale bars for all images are 10µm. A white line in the GFP control image shows the border between the SVZ (above) and VZ (below). 3B) Comparison of the percent of cells with an apical endfoot length (AEL) less than 15 µm in RGPs expressing GFP and phosphomutant forms of Nde1. 3C) Mitotic indices of phosphomutant constructs co-transfected with GFP. All statistical comparisons are made to control data. One-way ANOVA and post hoc Dunnet test were used in 3B-C), ns = not significant, *p<0.05, **p<0.01, ***p<0.001. n = mean of values across at least 3 different embryos from at least 2 different operations per condition. All experiments done with E16 operations and E20 analysis in developing rat brains. 3B-C) data plotted as interquartile range with 5-95% whisker range.

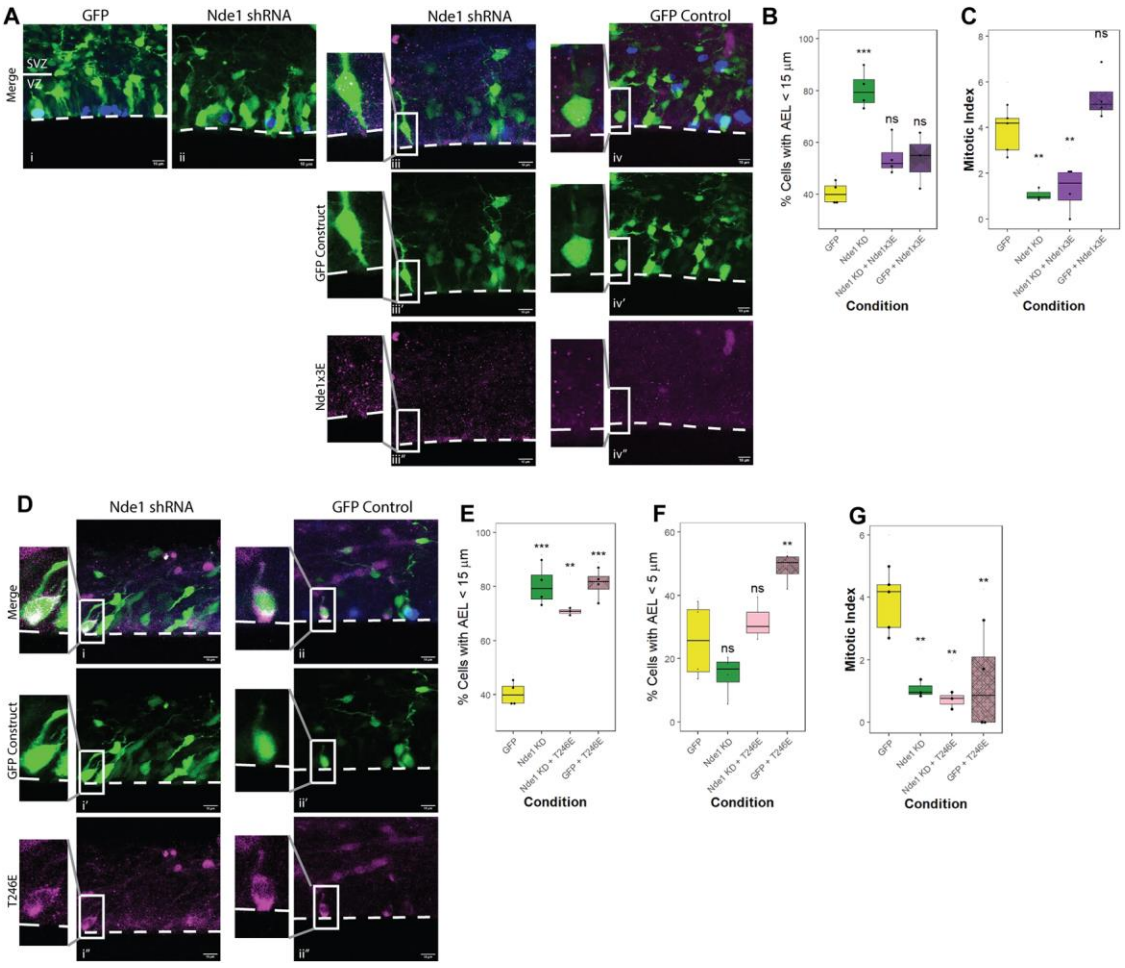

Figure 4. Effects of Nde1 phospho-mimetic constructs on INM and mitotic index
4A) Representative images of RGP cells in embryonic rat brain subjected to IUE with GFP control plasmid alone (i), Nde1 KD alone (ii), or Nde1x3E with Nde1 shRNA (iii) or GFP control (iv). In merged images (4Ai-iv), PH3 is shown in blue, GFP or Nde1 shRNA in green, and mCherry tagged Nde1x3E in magenta. GFP or Nde1 shRNA is shown alone in 4Aiii'-iv'. Nde1x3E is shown in magenta in 3Aiii''-iv'', with example cells enlarged adjacent to the full images. A white line in the GFP control image shows the border between the SVZ (above) and VZ (below) and a dashed white line in all images indicates the ventricular surface. 4B) Comparison of the percent of cells an apical endfoot length (AEL) less than 15 µm of the ventricular surface in RGPs expressing GFP, Nde1 shRNA, or Nde1x3E with GFP or Nde1 shRNA. 4C) Mitotic indices of RGPs expressing GFP, Nde1 shRNA, or Nde1x3E with GFP or Nde1 shRNA. 4D) Representative images of RGP cells in embryonic rat brain subjected to IUE with T246E in combination with Nde1 shRNA (i) or GFP control (ii). In merged images (4Di-ii), PH3 is shown in blue, GFP or Nde1 shRNA in green, and mCherry tagged T246E in magenta. GFP or Nde1 shRNA is shown alone in 4Di'-ii'. T246E is shown in magenta in 4Di''-ii'', with example cells enlarged adjacent to the full images. Scale bars for all images are 10µm. 4E) Comparison of the percent of cells an apical endfoot length (AEL) less than 15 µm of the ventricular surface in RGPs expressing GFP, Nde1 shRNA, or T246E with GFP or Nde1 shRNA.

4F) Comparison of the percent of cells an apical endfoot length (AEL) less than 5 μm of the ventricular surface in RGPs expressing GFP, Nde1 shRNA, or T246E with GFP or Nde1 shRNA 4G) Mitotic indices of RGPs expressing GFP, Nde1 shRNA, or T246E with GFP or Nde1 shRNA. All statistical comparisons are made to control data. One-way ANOVA and post hoc Dunnet test were used in 4B-C, E-G), ns = not significant, *p<0.05, **p<0.01, ***p<0.001. n = mean of values across at least 3 different embryos from at least 2 different operations per condition. All experiments done with E16 operations and E20 analysis in developing rat brains. 4B-C, E-G) data plotted as interquartile range with 5-95% whisker range.

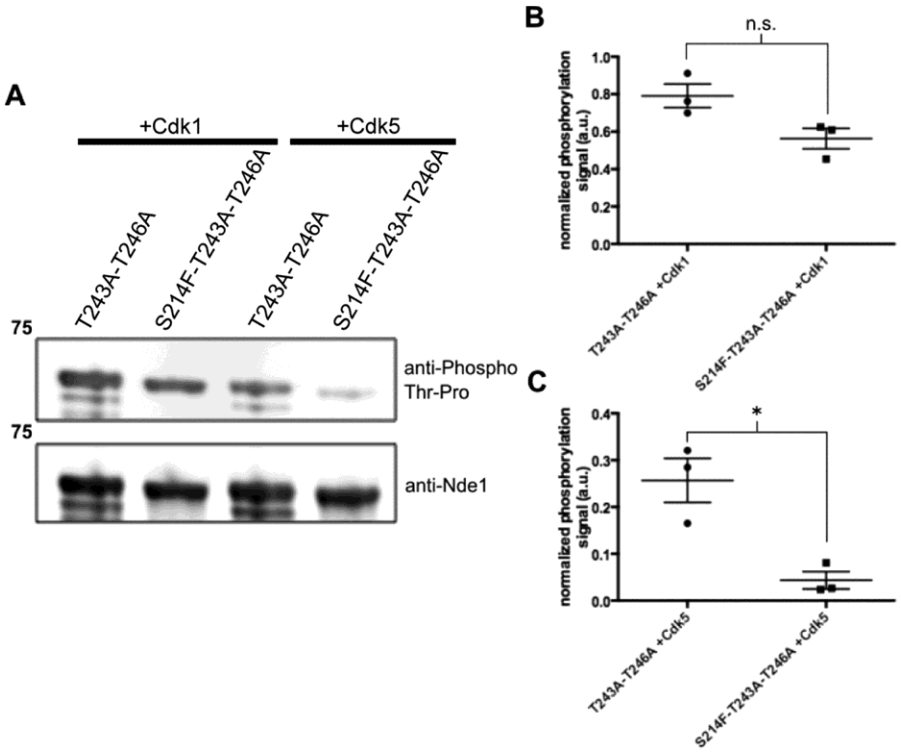

Figure 5 Phosphorylation of Nde1-S214F with Cdk1 and Cdk5
5A) The human NDE1-encoding cDNA with the S214F mutation in tandem with phosphomutation of the T243 and T246 sites from T to A were expressed and purified to isolate the effect of the S214F mutation on Cdk1 and Cdk5 phosphorylation. Multiple bands are commonly seen for Nde1, a single band is likely seen in the S214F condition due to conformational changes in the protein due to the substitution of a large hydrophobic residue for an uncharged residue. There is a clear reduction in Cdk5 phosphorylation in Nde1 with the S214F mutation, but no effect on Cdk1 phosphorylation. 5B-C) Quantification of the anti-phosphothreonine signal relative to the anti-Nde1 signal. Data plotted as mean with standard deviation. Comparison using paired t-test, *p<0.01.

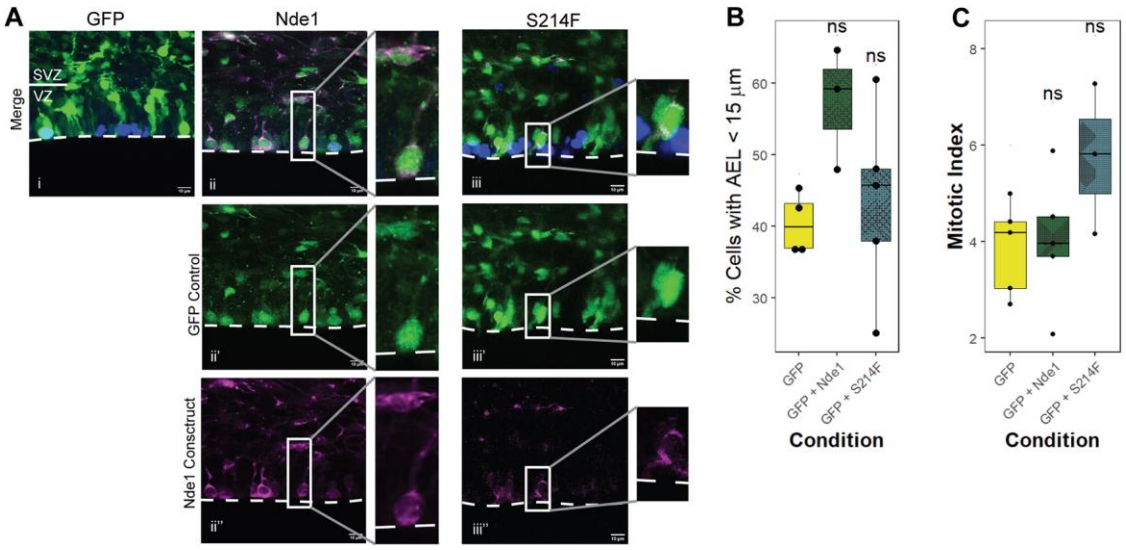

Figure 6. Effects of Schizophrenia associated mutation on RGPs
6A) Representative images of RGP cells embryonic rat brain subjected to IUE with GFP control plasmid alone (i), Nde1 with GFP control (ii), or S214F with GFP control (iii). In merged images (6Ai-iii), PH3 is shown in blue, GFP in green, and Nde1 constructs in magenta. GFP is shown alone in 6Aii'-iii'. mCherry tagged Nde1 or S214F is shown in magenta in 6Aii''-iii'', with example cells enlarged adjacent to the full images. A dashed white line in all images indicates the ventricular surface. Scale bars for all images are 10µm. 6B) Comparison of the percent of cells with an apical endfoot length (AEL) less than 15 µm of the ventricular surface in RGPs expressing GFP alone, and with Nde1 and S214F 6C) Mitotic indices of RGPs expressing GFP alone, and with Nde1 and S214F. All statistical comparisons are made to control data. One-way ANOVA and post hoc Dunnet test were used in 6B-C), ns = $p > 0.05$. n = mean of values across at least 3 different embryos from at least 2 different operations per condition. All experiments done with E16 operations and E20 analysis in developing rat brains. 6B-C) data plotted as interquartile range with 5-95% whisker range.

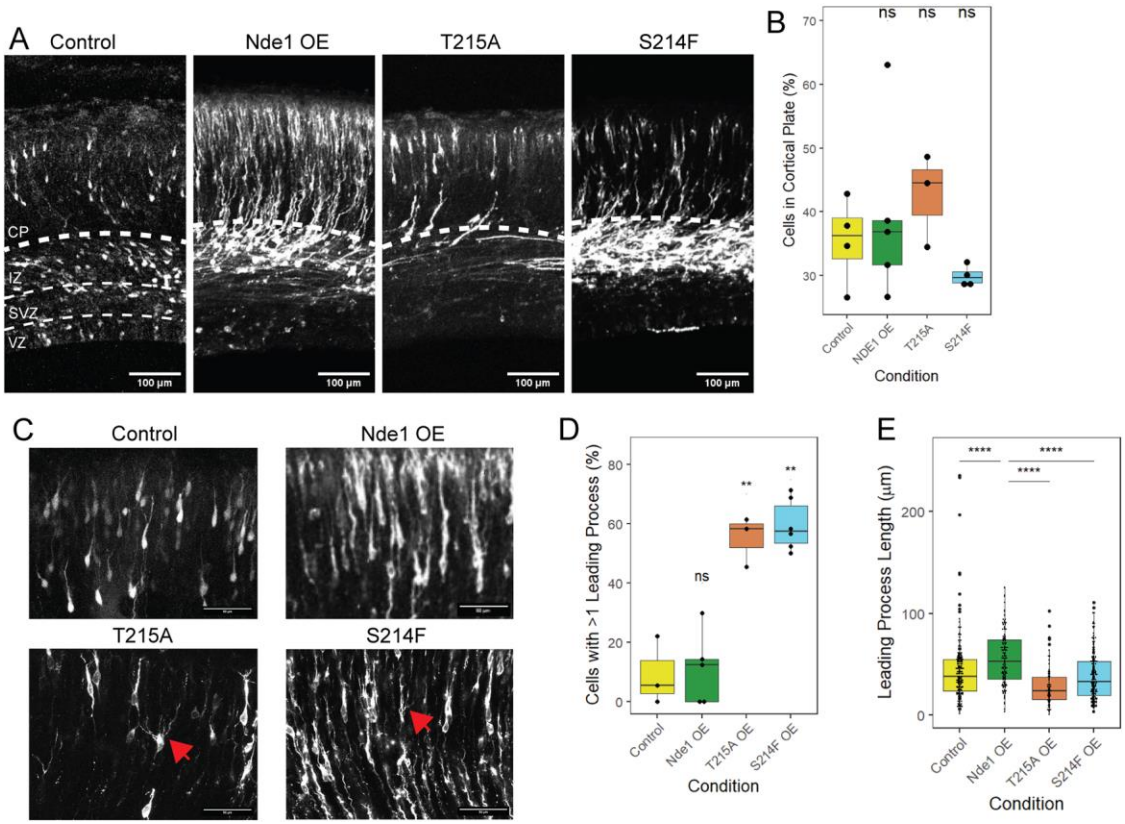

Figure 7. Effects of T214A and S214F Mutations on Neuronal Migration and Morphology
7A) Representative images of cortices expressing diffuse RFP alone (Control) or RFP in combination with untagged Nde1, T215A, or S214F. In the control image, the four regions of the cortex are indicated by dashed lines. In the other images, only the boundary between the cortical plate (CP) and the rest of the cortex is indicated. Scale bar = 100 µm. 7B) Quantification of the percent of transfected cells that reached the CP in each condition. 7C) Representative images of the neurons in the CP in cells expressing diffuse RFP alone or with Nde1, T215A, or S214F. Red arrows in the T215A and S214F images indicate neurons with >1 leading process. Scale bar = 50 µm 7D) Quantification of the percent of cells with >1 leading process in each condition. 7E) Quantification of the length of leading processes in each condition. Statistical comparisons in 7A and 7D are made to control data and to Nde1 OE in 7E. Unpaired t-test used in 7B and 7D. Kolmogorov-Smirnov test used in 7E. ns = $p > 0.05$, **$p<0.01$, ****$p<0.0001$. n = mean of values across at least 3 different embryos from at least 2 different operations per condition. All experiments done with E16 operations and E20 analysis in developing rat brains. 7B, 7D-E data plotted as interquartile range with 5-95% whisker range.

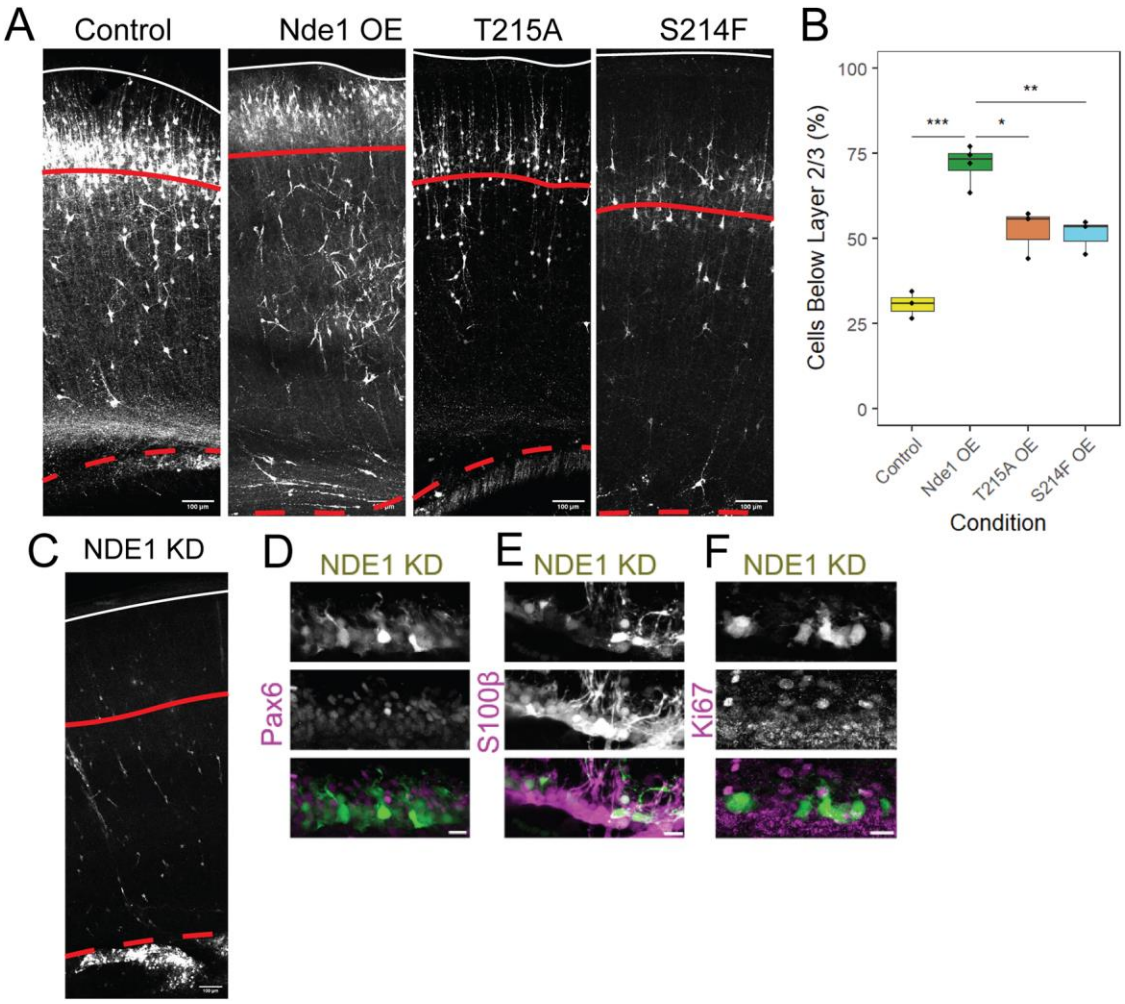

Figure 8. Effects of S214F Mutation on Neuronal Migration in Post-natal Brains
8A) Representative images of cells expressing diffuse RFP alone (Control) or RFP with untagged Nde1 OE, T215A, or S214F in P6 brains. Solid red line indicates the boundary of cortical layer 2/3, which was determined with Cux1 staining. Solid white line indicates the pial surface and red dashed line indicates the boundary of the white matter. Scale bar = 100 μm 8B) Quantification of the percent of cells below the layer 2/3 boundary in each condition. 8C) Representative image of a P6 brain expressing Nde1 KD. Scale bar = 100 μm 8D-F) Representative images of cells in a P6 brain expressing Nde1 KD (green in merged image) as well as proliferative markers Pax 6 (8D), S100β (8E), or Ki67 (8F), shown in magenta in merged images. Scale bar = 10 μm. Unpaired t-test used in 8B. *p<0.05, **p<0.01, ***p<0.001. n = mean of values across at least 3 different brains from at least 2 different operations per condition. All experiments done with E16 operations and P6 analysis. 8B data plotted as interquartile range with 5-95% whisker range.

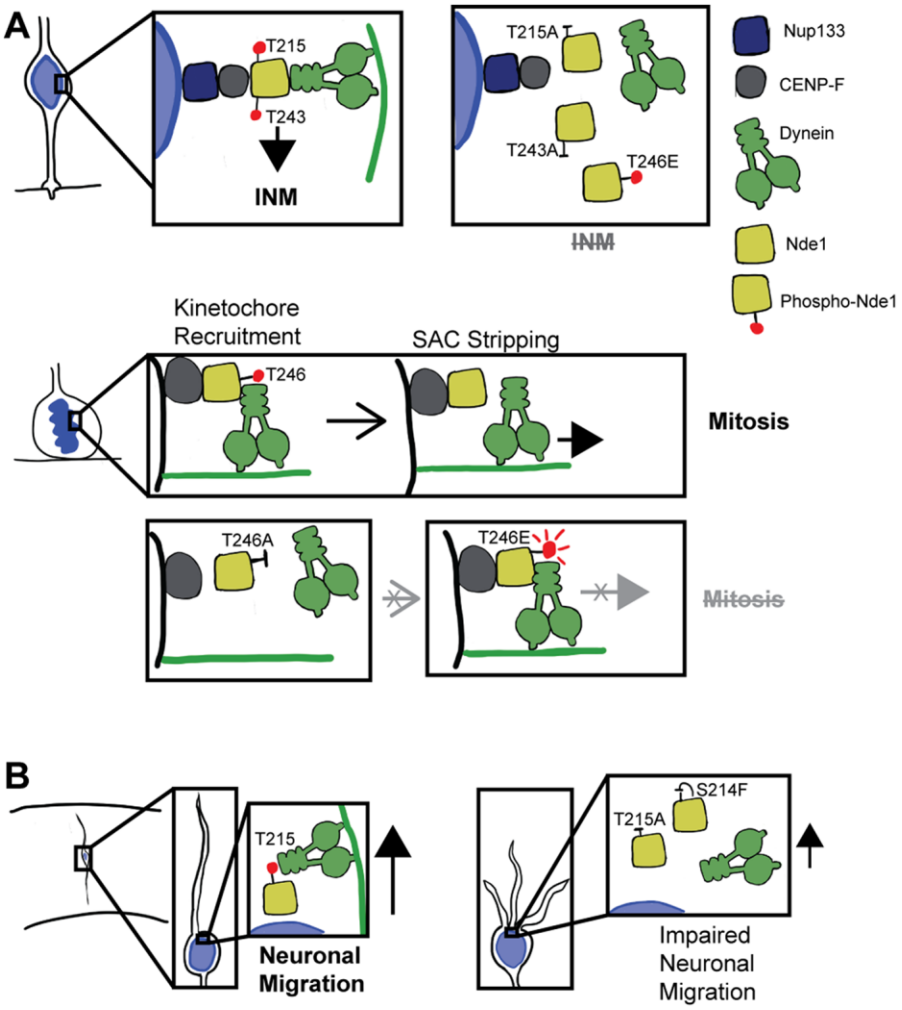

Figure 9. Model of Nde1 phosphorylation sites and their effects on INM and mitotic entry
9A) Proposed model for Cdk1 mediated Nde1 phosphorylation in RGPs during INM (top) and mitosis (bottom). Top: T215 and T243 must be phosphorylated during late G2 in order to recruit dynein and complete INM. Mutations T215A, T243A, and T246E inhibit this process. Bottom: CENP-F and Nde1 interact at kinetochores during mitosis. As both T246A and T246E inhibit this process, a possible model is one in which Nde1 phosphorylation at T246 is required for recruitment to kinetochores, while the same residue must be dephosphorylated in order to release dynein from kinetochores to strip spindle assembly checkpoint (SAC) proteins from the kinetochore corona for mitosis to proceed. 9B) Proposed model for Cdk5 function in post-mitotic neuronal migration. T215 must be phosphorylated in order for effective neuronal migration and cell morphology. Mutations T215A and S214F both impair this process and alter cell morphology.